HBRC Journal (2015) **11**, 201–212

Housing and Building National Research Center

HBRC Journal

http://ees.elsevier.com/hbrcj

Behavior of reinforced concrete columns strengthened by steel jacket

Mahmoud F. Belal [a], **Hatem M. Mohamed** [b,*], **Sherif A. Morad** [b]

[a] *Higher Technological Institute, 10th of Ramadan City, Egypt*
[b] *Faculty of Engineering, Cairo University, Cairo, Egypt*

Received 29 December 2013; revised 5 May 2014; accepted 19 May 2014

KEYWORDS

RC columns;
Strengthening;
Retrofitting;
Steel jacket;
F.E analysis;
Experimental testing

Abstract RC columns often need strengthening to increase their capacity to sustain the applied load. This research investigates the behavior of RC columns strengthened using steel jacket technique. Three variables were considered; shape of main strengthening system (using angles, C-sections and plates), size and number of batten plates. Behavior and failure load of the strengthened columns were experimentally investigated on seven specimens divided into two un-strengthened specimen and five strengthened ones. A finite element model was developed to study the behavior of these columns. The model was verified and tuned using the experimental results. The research demonstrated that the different strengthening schemes have a major impact on the column capacity. The size of the batten plates had significant effect on the failure load for specimens strengthened with angles, whereas the number of batten plates was more effective for specimens strengthened with C-channels. Then, by using finite element (F.E) package ANSYS 12.0 [1] their behavior was investigated, analyzed and verified. Test result showed a good match between both experimental tests and F.E models.

Introduction

Reinforced concrete structures often require strengthening to increase their capacity to sustain loads. This strengthening may be necessary due to change in use that resulted in additional live loads (like change in use of the facility from residential to public or storage), deterioration of the load carrying elements, design errors, construction problems during erection, aging of structure itself or upgrading to confirm to current code requirements (seismic for example). These situations may require additional concrete elements or the entire concrete structure to be strengthened, repaired or retrofitted. Common methods for strengthening columns include concrete jacketing, fiber reinforced polymer (FRP) jacketing and steel jacketing. All these methods have been shown to effectively increase the axial load capacity of columns.

Julio Garzón-Rocaet et al. [2] presented the results of a series of experimental tests on full-scale specimens strengthened with steel caging including simulation of the beam-column

* Corresponding author. Tel.: +201223185801; fax: +202330424645.
E-mail address: hatem_amn@yahoo.com (H.M. Mohamed).
Peer review under responsibility of Housing and Building National Research Center.

Production and hosting by Elsevier

1687-4048 © 2014 Production and hosting by Elsevier B.V. on behalf of Housing and Building National Research Center.
http://dx.doi.org/10.1016/j.hbrcj.2014.05.002

joint under combined bending and axial loads. Capitals were applied to all the specimens to connect the caging with the beam-column joint either by chemical anchors or steel bars. It was observed that steel caging increases both the failure load and ductility of the strengthened columns.

Khair Al-Deen Isam Bsisu [3] performed an experimental and theoretical study on 20 square reinforced concrete columns retrofitted with steel jacket technique. All tested specimens were tested under concentric axial loading. The author concluded that retrofitting square reinforced concrete columns with full steel jackets enhanced the compressive strength more than double the strength of the original column without retrofitting. Also, confinement of reinforced concrete columns with steel jackets enhanced the ductility of the column.

Pasala Nagaprasad et al. [4] presented a rational design method to proportion the steel cage considering its confinement effect on the concrete column. An experimental study was carried out to verify the effectiveness of the proposed design method and detailing of steel cage battens within potential plastic hinge regions. The author concluded that the performance of deficient RC columns under combined axial and cyclic lateral loading can be greatly improved by steel caging technique without using any binder material in the gap between concrete column and steel angles. The proposed design method was found effective and reasonably accurate. Detailing of end battens of the steel cage located in the potential plastic hinge region played an important role in improving the column overall behavior under lateral loads. The increase in width of end battens significantly enhanced the plastic rotational capacity and its resistance to lateral loads; however, it had a minor effect on the overall energy dissipation potential.

Rosario Montuori et al. [5] presented a theoretical model to predict the moment curvature behavior of RC columns confined by angles and battens and the validation of the proposed model by results from experimental testing on 13 specimens tested under axial force. It was concluded that theoretical model showed a good ability to predict the behavior of columns strengthened with angles and battens in terms of both deformation and resistance.

The objective of this research program is to determine the effect of the following parameters on the behavior of strengthened RC column: shape of main strengthening system (using angles, C-sections and plates), size, and number of confining batten plates. A comparison is made between the experimental test results and analytical results obtained through the finite element program ANSYS 12.0 [1].

Experimental testing

In order to investigate the effect of the above mentioned parameters on the behavior of strengthened RC column, an experimental program was carried out to test seven RC columns with concrete compressive strength of $f_{cu} = 34\ \mathrm{N/mm^2}$.

Test specimens

All tested columns were 200×200 mm in cross-section with 1200 mm height .The specimens were divided into two groups: the first group includes two control specimens without strengthening and second group includes five specimens strengthened with different steel jacket configurations. Vertical steel elements (angles, channel and plates) were chosen to have the same total horizontal cross sectional area. Table 1 gives the reinforced concrete column data for all specimens while Table 2 gives strengthening details for each specimen. Fig. 1 shows specimens' dimensions and steel jacket configuration while Fig. 2 shows the strengthened specimens after casting and jacket erection.

Concrete mix and casting

The concrete mix used for grade 34 Mpa is shown in Table 3. The concrete mixture used was prepared from ordinary Portland cement, natural sand and crushed natural dolomite aggregate with maximum nominal size of 10 mm. The test specimens were vertically cast in wooden forms stiffened by battens to maintain the form and shape.

Test procedure

The specimens were placed in the testing machine between the jack head and the steel frame. The strain gages, load cell and linear voltage displacement transducer (LVDT) were all connected to the data acquisition system attached to the computer. The load was monitored by a load cell of 5000 kN capacity and transmitted to the reinforced concrete column through steel plates to provide uniform bearing surfaces. Fig. 3 shows a schematic view of the test setup. A controlled data acquisition system was used to continuously record readings of the electrical load cell, the two dial gauges of 0.01 mm accuracy (LVDT instruments) that measure the column horizontal deformations in two perpendicular directions, the reinforcement strain gages and also the steel jacket

Table 1 Reinforced concrete column data for all specimens.

Specimen	f_{cu} (N/mm^2)	Dimensions (mm)	RFT		
			Long bars		Stirrups
			Type	f_y (N/mm^2)	
Col.00 (2 specimens) Col.01.L.3P Col.02.L.6P Col.03.C.3P Col.04.C.6P Col.05.Pl	34	$200 \times 200 \times 1200$	4 Φ 12 mm @ corners	360 N/mm^2	6 φ 8/m‘

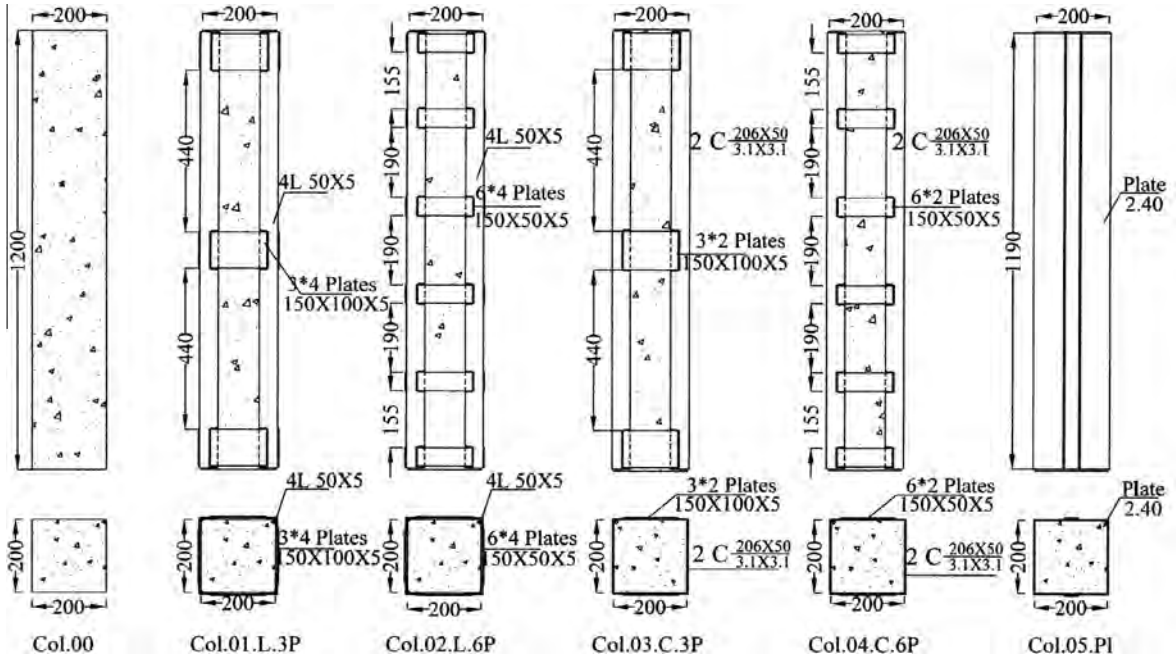

Fig. 1 Specimen dimensions and steel jacket configuration.

Table 2 Strengthening details for each specimen.

Specimen	Strengthening configuration			
	Type	Size (mm)	Confinement	
			Original	Additional
Col.00 (2 specimen)	Reference specimens (Refs. [1,2])			
Col.01.L.3P	Angles	4 L 50*50*5	3*4 plates 150*100*2	–
Col.02.L.6P	Angles	4 L 50*50*5	3*4 plates 150*50*2	3*4 plates 150*50*2
Col.03.C.3P	Channels	2C (206*50)/(3.1*3.1)	3*4 plates 150*100*2	–
Col.04.C.6P	Channels	2C (206*50)/(3.1*3.1)	3*4 plates 150*50*2	3*4 plates 150*50*2
Col.05.Pl	Plates	4 Plates @ 4 sides	4*4 plates 200*2.4	–

Fig. 2 Strenthened specimens after casting and jacket erection.

strain gages. To ensure that failure will occur in the specimen's body not the head, the top and bottom ends of the specimens

Table 3 Concrete mixing proportions in kN.

Cement	Water	Aggregates	Sand	w/c ratio
360	180	1200	600	0.50

were more confined with steel boxes made from 10-mm thick steel plates. All test records were automatically saved on computer file for further data manipulation and plotting. All tests were conducted in The Material laboratory of Housing and Building National Research Center (HBRC).

Analytical work using finite element model

The finite element package ANSYS 12.0 [1] was used to simulate the experimental testing by introducing a numerical model. The tested columns in the experimental work were modeled to determine the failure loads and strains in each specimen. Comparison of results between experimental and F.E was carried out.

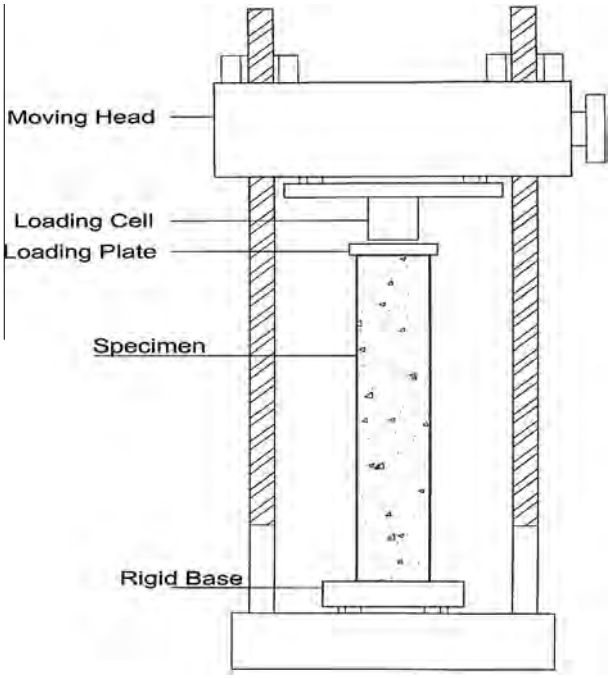

Fig. 3 Schematic view of the test setup.

Defining material properties

Concrete stress strain relationship

The Solid 65 element defining concrete requires linear isotropic and multi-linear isotropic material properties to properly model concrete [6,7]. The multi-linear isotropic material uses the following equations to compute the multi-linear isotropic stress–strain curve for the concrete [8].

$$f = E_c^* \varepsilon / [1 + (\varepsilon/\varepsilon_0)^2] \quad (1)$$

$$\varepsilon_0 = 2^* f_c' / E_c \quad (2)$$

$$E_c = f/\varepsilon \quad (3)$$

Where:

f = stress at any strain ε, psi
ε = strain at stress f
ε_0 = strain at the ultimate compressive strength f_c'

The multi-linear isotropic stress–strain implemented requires the first point of the curve to be defined by the user. It must satisfy Hooke's Law.

Fig. 4 shows the stress–strain relationship proposed for this study. This curve was proposed by Kachlakev, et al. [8] which is defined by 5 points as follows:

Point no.1, defined at 0.30 f_c', is calculated for the stress–strain relationship of concrete in the linear range (Eq. 3).

Point nos. 2, 3, and 4 are calculated from (Eq. 1) with ε_0 obtained from (Eq. 2). Strains were selected and the stress was calculated for each strain.

Point 5 is defined at f_c and ε_0 indicating traditional crushing strain for unconfined concrete.

Fig. 5 shows the stress–strain relationship calculated using Eqs. (1)–(3).

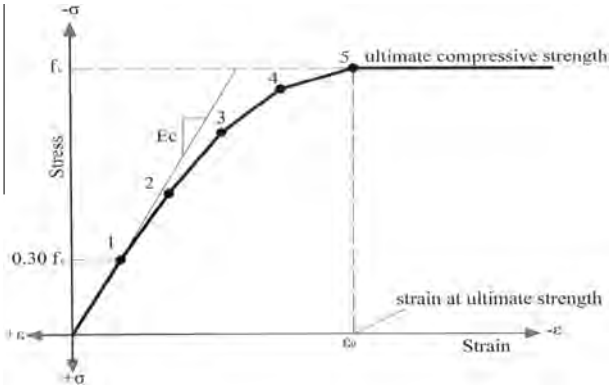

Fig. 4 Uniaxial stress–strain curve [8].

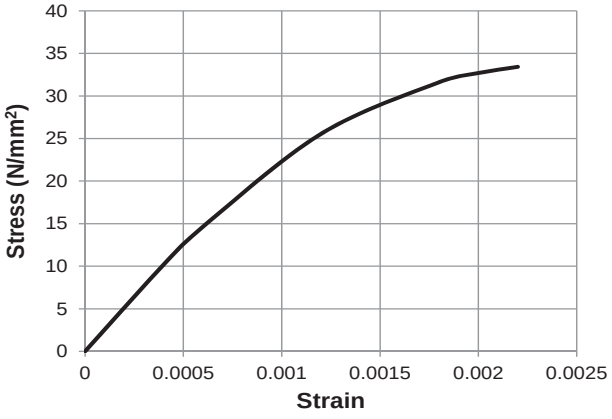

Fig. 5 Calculated stress–strain relationship for concrete.

Implementation of material model

Implementation of material model requires different constants to be defined. Typical shear transfer coefficients range from 0.0 to 1.0, with 0.0 representing a smooth crack (complete loss of shear transfer) and 1.0 representing a rough crack (no loss of shear transfer). The shear transfer coefficients for open and closed cracks were determined by Kachlakev, et al. [8] as a basis. Convergence problems occurred when the shear transfer coefficient for the open crack dropped below 0.20 [8].

The uniaxial cracking stress was calculated based upon the modulus of rupture. This value is determined using Eq. 4.

$$f_r 0.60^* \sqrt{f_c'} \quad (4)$$

The uniaxial crushing stress in this model was based on the uniaxial unconfined compressive strength f_c'.

Table 4 Summary data for specimen materials.

Item	Element type	Material number	Real constant number
Concrete	Solid 65	1	1
Long. bars	Link 8	2	2
Trans. bars	Link 8	3	3
Steel plates and sections	Solid 45	4	–

Table 5 Material properties for each element.

Material number	Element type	Material properties	
1	Solid 65	Concrete (linear isotropic properties)	
		E_x	25238.79 N/mm^2
		Poisson's ratio (PRXY)	0.200
		Concrete (multi-linear isotropic properties)	
		Shear coefficient for open shear	0.20
		Shear coefficient for closed shear	0.80
		Uniaxial tensile stress (N/mm^2)	3.4
		Uniaxial crushing stress (N/mm^2)	34
		Biaxial crushing stress (N/mm^2)	0
		Ambient hydrostatic stress state (N/mm^2)	0
		Biaxial crushing stress under ambient hydrostatic stress state (N/mm^2)	0
		Uniaxial crushing stress under ambient hydrostatic stress state (N/mm^2)	0
		Stiffness multiplier for cracked tensile condition	0
2	Link 8	Longitudinal bars	
		Linear isotropic	
		E_x	2.1*10^5 N/mm^2
		Poisson's ratio (PRXY)	0.300
		Bilinear isotropic	
		Yield stress	360 N/mm^2
		Tangent modulus	0.000
3	Link 8	Transverse bars	
		Linear isotropic	
		E_x	2.1*10^5 N/mm2
		Poisson's ratio (PRXY)	0.300
		Bilinear isotropic	
		Yield stress	240 N/mm2
		Tangent modulus	0.000
4	Solid 45	Steel plates and sections	
		Linear isotropic	
		E_x	2.1*105 N/mm2
		Poisson's ratio (PRXY)	0.300

Summary of specimen item and corresponding element type, material number and real constant number are given in Table 4 while the material properties for each used element are shown in Table 5.

Building the model

Figs. 6–11 show models' geometry after building. Half the column height is considered during creating the models for all specimens benefiting from the column symmetry and taking into account the correct simulation of the boundary conditions and loads.

Boundary conditions and loads

The boundary conditions were chosen to simulate the experimental conditions. The horizontal translations of all base joints were restrained in the three directions. Figs. 12 and 13 show boundary conditions and method of loading of specimen respectively.

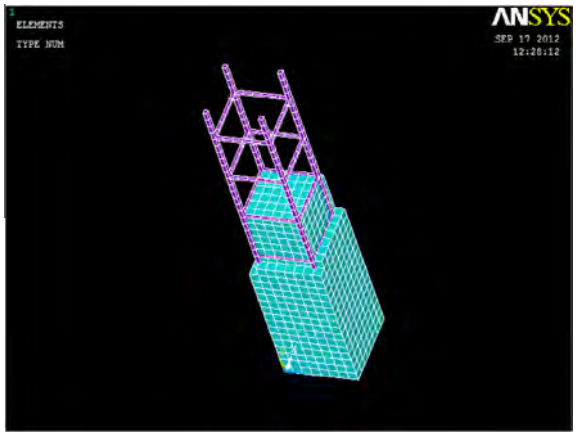

Fig. 6 Model for specimen Col.00.

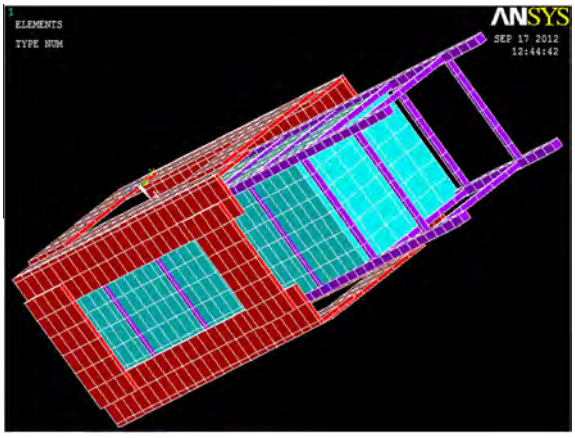

Fig. 7 Model for specimen Col.01.4L.3P.

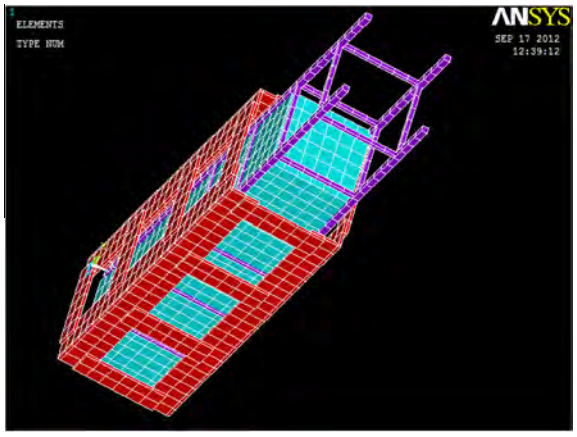

Fig. 8 Model for specimen Col.02.4L.6P.

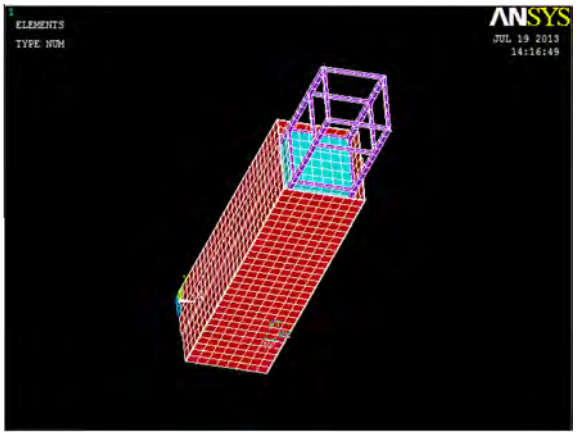

Fig. 11 Model for specimen Col.05.Pl.

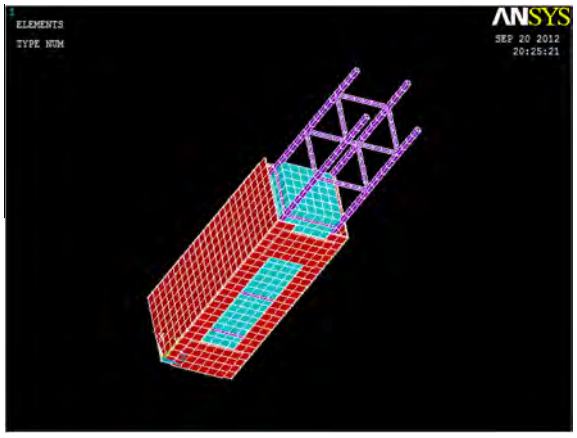

Fig. 9 Model for specimen Col.03.C.3P.

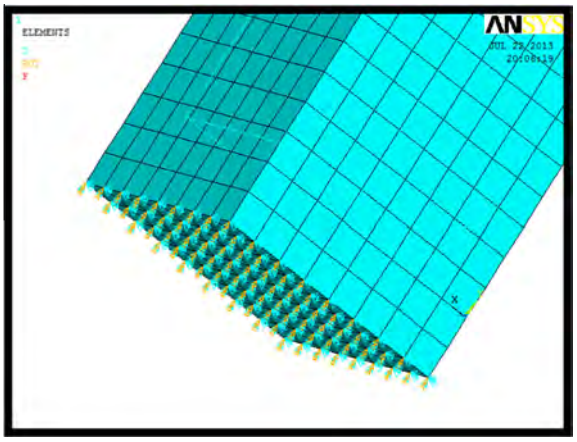

Fig. 12 Boundary conditions.

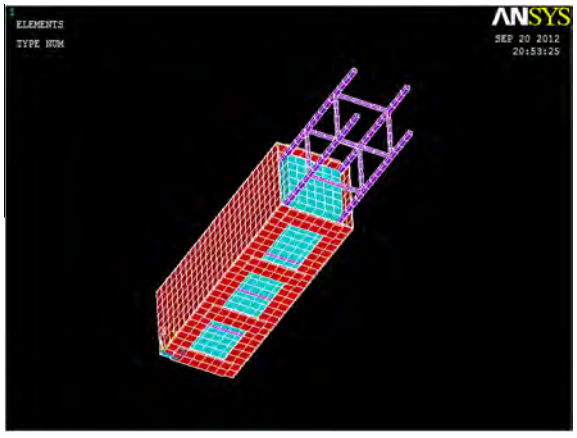

Fig. 10 Model for specimen Col.04.C.6P.

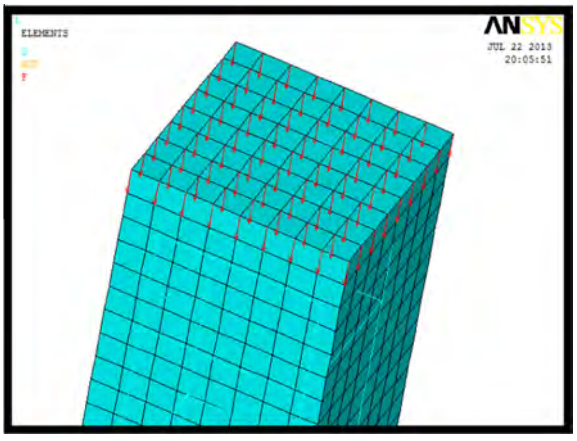

Fig. 13 Loading specimen.

Test results

Experimental results

Modes of failure and failure loads

Modes of failure and failure loads varied depending on the configuration of steel jacket as well as its arrangement. Because the strengthening elements covered most of specimen, it was not possible to observe either the initial cracks or the cracking load for specimens. So, only failure load was recorded. Failure load is considered the maximum recorded load during testing and at which specimen could not carry any extra load. Table 6 gives the failure loads for all specimens

Table 6 Failure loads for all specimens.

Specimen	Failure load P_u (kN)	$P_u/P_{u(Ref.)}$
Col.00 (Ref.)	1255	1.00
Col.01.L.3P	1821	1.45
Col.02.L.6P	1649	1.31
Col.03.C.3P	1545	1.23
Col.04.C.6P	1841	1.47
Col.05.Pl	1489	1.19

and the percentage of increase with respect to reference specimen (Col.00) while Fig. 14 focuses on the damage observed in each specimen at failure.

Specimen Col.00. Behavior of both reference columns was similar. As the load increased, inclined cracks started to appear near the upper part of the column head. The cracks increased in number and became wider with the increase of the load. At approximate 92% of the failure load of the column (1140 kN), concrete cover spalled off and a visible buckling of longitudinal reinforcement with outside buckling in the transverse reinforcement (stirrups) occurred from one side as shown in Fig. 14a. When the load reached 1250 kN, crushing damage was observed and total collapse of specimen occurred.

Specimen Col.01.L.3P. As the load increased, small cracks started to appear just under the loading plate. Further increase in the load resulted in major cracks in the lower part of column. Then at approximate 98% of the failure load (1780 kN), concrete cover started to spall off, revealing buckling in both vertical reinforcement and corner angles. At

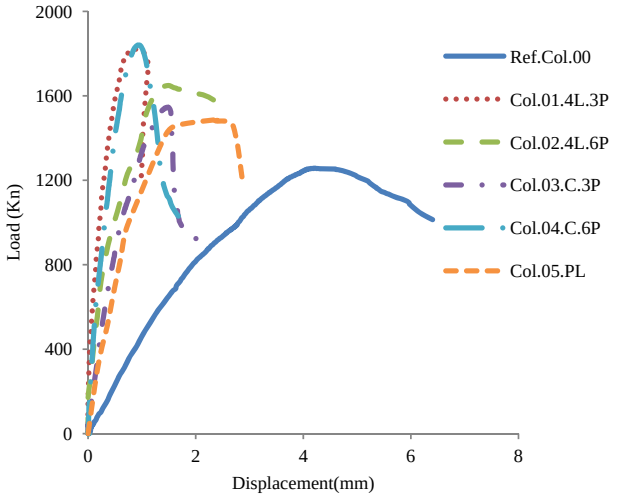

Fig. 15 Load–displacement relationship for all specimens.

(a) Specimen Col.00

(b)Specimen Col.01.L.3P

(c)Specimen Col.02.L.6P

(d) Specimen Col.03.C.3P

(e)Specimen Col.04.C.6P

(f)Specimen Col.05. PL

Fig. 14 Failure in all tested specimens.

Table 7 Failure load and the corresponding displacement for all specimens.

Specimen	Failure load P_u (kN)	Disp. δ (mm)	$\delta/\delta_{ref.}$
Col.00 (Ref. specimen)	1255	4.24	1.00
Col.01.L.3P	1821	0.89	0.21
Col.02.L.6P	1649	1.55	0.37
Col.03.C.3P	1545	1.46	0.35
Col.04.C.6P	1841	0.93	0.22
Col.05.Pl	1489	2.45	0.58

failure load (1821 kN), the welding of the bottom batten plate ripped off because of the lateral expansion of concrete as shown in Fig. 14b causing an explosion sound.

Specimen Col.02.L.6P. This specimen started with minor cracks located under loading plate. In the bottom part of column, major cracks were formed because of concrete lateral expansion. As the load increased, cover spalled off and the welding of the two batten plates located at bottom ripped off. This occurred at approximate 1649 kN as shown in Fig. 14c.

Specimen Col.03.C.3P. Typical small inclined cracks appeared in the upper part of column under loading plate. The cracks increased in number and became wider with the increase of the load. At approximate 1480 kN a noticeable buckling occurred in one flange of the jacket and its web accompanied with major crack causing cover to spall off .Finally, the specimen failed at about 1545 kN as shown in Fig. 14d.

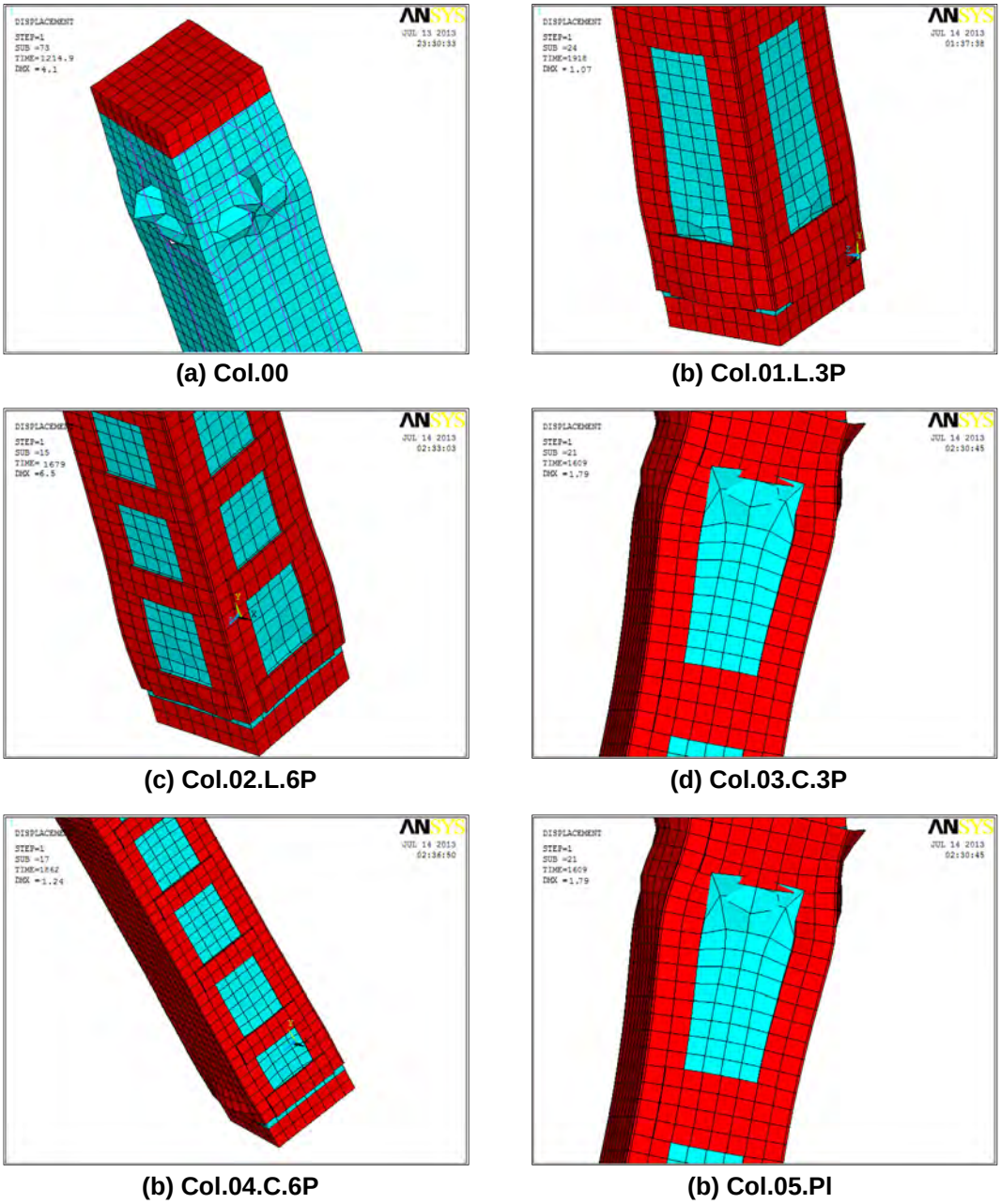

Fig. 16 Deformation of all models at failure load.

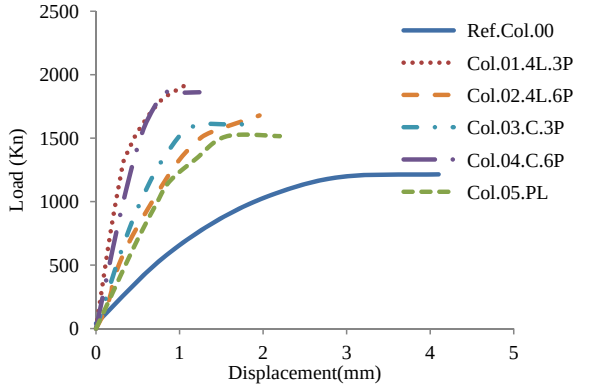

Fig. 17 Load–displacement relationship for all models.

Table 8 Failure load and the corresponding displacement using finite elements.

Specimen	Failure Load P_u (kN)	Disp. δ (mm)
Col.00 (Ref. specimen)	1215	4.10
Col.01.L.3P	1918	1.07
Col.02.L.6P	1679	1.96
Col.03.C.3P	1609	1.79
Col.04.C.6P	1862	1.24
Col.05.Pl	1516	2.20

Specimen Col.04.C.6P. Typical small inclined cracks appeared in the upper part of column under loading plate. As the load increased, major cracks start to appear in lower part and became wider causing the cover to spall off revealing reinforcement. Finally, the specimen failed at approximate 1841 kN with a minor buckling in bottom batten plates and channel flange as shown in Fig. 14e.

Specimen Col.05.Pl. This specimen was strengthened using steel plates covering all faces of the column and connected together with vertical plates. So, it was not possible to monitor neither concrete cracks nor reinforcement behavior "whether it buckled or not". At the test end, a remarkable buckling occurred at one side of specimen in the upper part while a slight one occurred at another side causing failure as shown in Fig. 14f.

Factors affecting failure load

Shape of steel jacket

All strengthened specimen have the same cross sectional area and improved the load carrying capacity compared to the reference specimen. Specimens Col.04.C.6P and Col.01 L.3P gave the highest failure load of 1841 kN and 1821 kN, respectively, corresponding to an increase of 47% and 45% as compared to the reference specimen. Specimen Col.02.L.6P failed only at 1649 kN with an increase not more than 31% and specimen Col.03.C.3P recorded only 1545 kN (23% increase) while specimen Col.05.PL gave the lowest value for strengthened one with 1489 kN (only 19% increase). As noticed, the specimen entitled "PL" has thinner plate thickness than other strengthened specimens "4L and 2C series", thus a large deformation and buckling occurs in it. The same behavior was noticed in specimen Col.03.C.3P which has a large deformation in the upper end of specimen.

Number and size of batten plates

Batten plates used to connect the steel elements (2C or 4L) were chosen to have the same cross sectional area. Three 150*100*5 mm plates were used for two specimens and six 150*50*5 mm plates were used for the other two.

For the columns strengthened with four angles, the increase in the size of batten plates increased the column capacity, due to the improvement in confining stress. The failure mode included buckling of the angles as well as local buckling of reinforcement bars between the batten pates.

Numbers of plates have a good effect on failure load in 2C series, increasing number of plates from 3 to 6 improved failure loads significantly. This is because of the continuity of the channel section all over the specimen height in two faces which protected the specimen from spalling by increasing the confinement especially at the bottom part of the column.

Factors affecting load displacement relationship

Load displacement relationship was drawn for each specimen during testing. Fig. 15 presents load versus experimental displacement curves for all tested specimens. Table 7 gives the failure loads with the corresponding measured displacement. It also provided the ratio between strengthened specimen displacement just before failure and that for reference specimen (Col.00).

All strengthened specimens failed at a lower value of displacement than the reference specimen. Fig. 15 shows the load–displacement curves for all specimens. All specimens behaved linearly up to about 50% of their failure load. For Col.00 specimen, displacement was 4.24 mm. For strengthened specimen, specimen Col.01.L.3P showed least displacement value of 0.89 mm which is 21% of that recorded for reference specimen. Also, specimen Col.04.C.6P gave a displacement of 0.93 mm which was 22% of reference specimen displacement. The displacement increased for specimens Col.02.L.6P and

Table 9 Comparison of failure load for all models.

Model	Failure load P_u (kN)		$P_{EXP}/P_{F.E.}$	Displacement δ (mm)		$\delta_{EXP}/\delta_{F.E.}$
	EXP.	F.E.		EXP.	F.E.	
Col.00 (Ref.)	1255	1215	1.03	4.24	4.10	1.03
Col.01.L.3P	1821	1918	0.95	0.89	1.07	0.83
Col.02.L.6P	1649	1679	0.98	1.55	1.96	0.79
Col.03.C.3P	1545	1609	0.96	1.46	1.79	0.82
Col.04.C.6P	1841	1862	0.99	0.93	1.24	0.75
Col.05.Pl	1489	1516	0.98	2.45	2.20	1.11

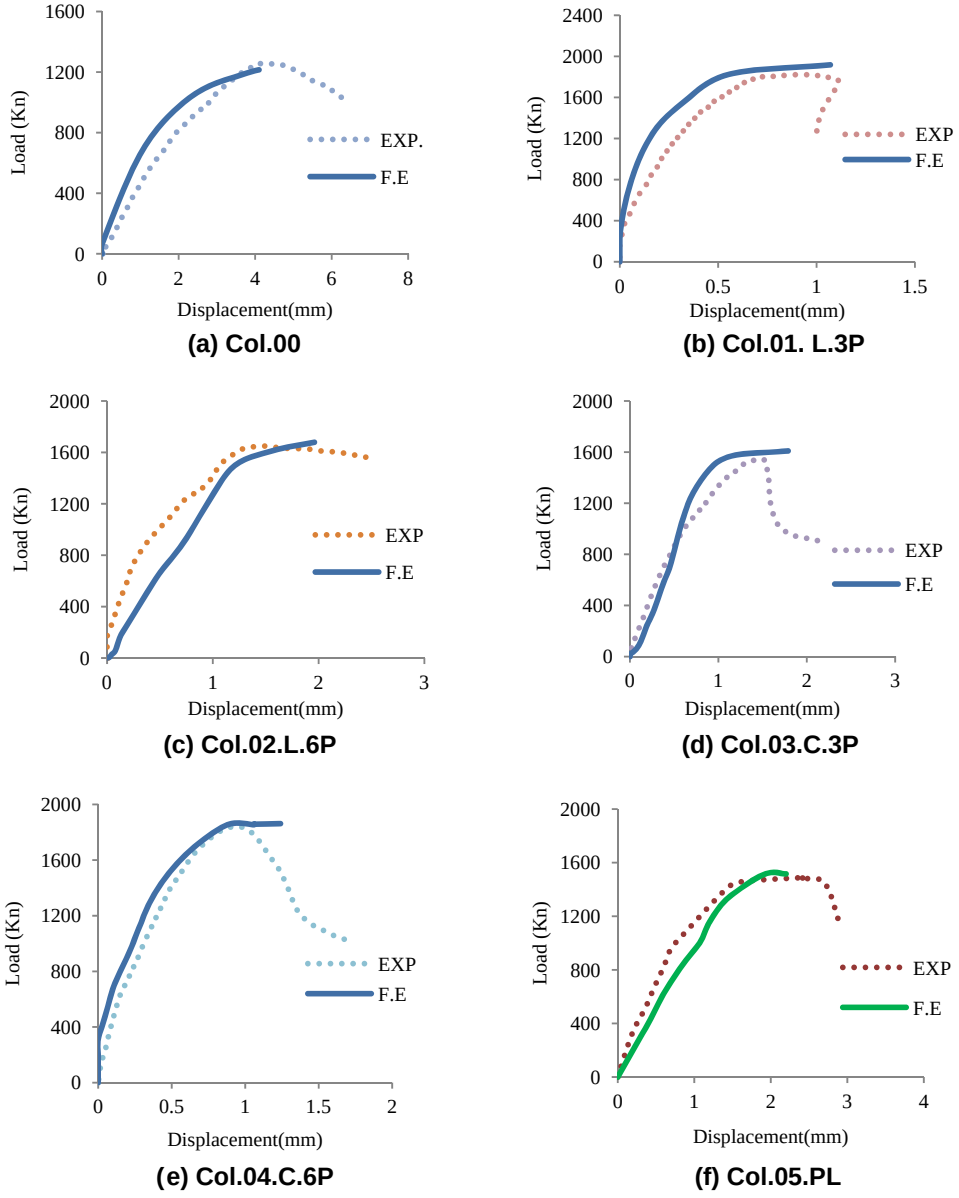

Fig. 18 Load–displacement relationship obtained from both experimental and analytical results.

Col.03.C.3P and reached 1.55 and 1.46 mm, respectively which is 37% and 35% of reference specimen displacement. Specimen Col.05.Pl gave the highest value with 2.45 mm which was 58% of reference specimen.

Effect of shape of steel jacket

To discuss the effect of each parameter on the lateral displacement, it is preferable to compare between specimens in a specific load value and the corresponding displacement. As noticed from Fig. 15, when comparing between specimens at load value of 1255 kN (failure load of Reference specimen Col.00), the displacements for specimens Col.01.L.3P, Col.02.L.6P, Col.03.C.3P, Col.04.C.6P and Col.01.Pl are 0.18, 1.00, 0.70, 0.36 and 1.37 mm, respectively. As noticed, the average 4 angles strengthened specimens displacement is 0.59 mm while that for channel strengthened specimens displacement is 0.53 mm which means that strengthening using angles or channels has a minor effect on the lateral displacement. However, using only steel plates for strengthening is not recommended since it increases the displacement by about 246% than that for strengthening using either angles or channels.

Effect of number and size of batten plates

It can be observed from Fig. 15 and Table 7 that the effect of number of batten plates on the load–displacement relationship depends on the shape of the main vertical steel element. For 2C series, specimen Col.04.C.6P gave a lower displacement than specimen Col.03.C.3P by about 36%. For 4L series, specimen Col.02.L.6P gave a higher displacement than specimen Col.01.L.3P by about 11%. This phenomenon requires further testing in order to properly investigate the effect of the batten plates.

Analytical results

Modes of failure

Behavior of numerical models for all specimens including cracks, deformed shapes and failure loads was recorded. It was noticed that cracked/crushed concrete elements were located in the area near column head while cracks have less concentration near the middle of the column height. Fig. 16 shows the deformation of all models at failure load.

Deformed shapes shown in Fig. 16 illustrate failure location in models for both concrete and steel jacket. In 4L series, deformation for both models was in the lower part of column; also in this part concrete elements were crushed causing a failure in the column. In 2C series, Col.03.C.3P had a large deformation in concrete and a noticeable buckling in steel jacket and batten plate in the upper part of column, while the Col.04.C.6P failed in the lower part with concrete element crushing and buckling in steel jacket. Model Col.05.Pl failed in upper part by a large deformation in steel jacket combined with crushing in concrete element. In all models; cracks started to develop in elements located just under loading plates. As the load increased, the cracks increased in number and width.

Load displacement relationships and failure loads

Fig. 17 gives the load–displacement relationships for all modeled specimens. Table 8 gives the failure loads with the corresponding measured displacement.

As in experimental results, all strengthened models gave higher loads than reference one. Reference model (Col.00) failed at the lowest load (1215 kN) combined with the largest displacement value of 4.10 mm. Strengthened model (Col.01.L.3P) failed at 1918 kN which was higher than reference one by 58% with 1.07 mm displacement which equals 26% of that for reference specimen. Model Col.02.L.6P recorded only 1679 kN as failure load which was higher than reference one by 38% and 1.96 mm as displacement (48% of reference specimen). Model (Col.03.C.3P) failed at a load of 1609 kN which was higher than that for reference by 32% at a displacement of 1.79 mm which equal 44% of reference model. Model Col.04.C.6P's failure load was 1862 kN which means 53% increase in the failure load occurred when compared with the reference model. Its recorded displacement was 1.24 mm which was 30% of the reference model. Finally, model Col.05.Pl gave 1516 kN as failure load which was higher than reference by 25% and 2.20 mm as displacement which was 54% of reference value.

Comparison between experimental and analytical finite elements results

Table 9 shows the failure loads and their corresponding displacement for both experimental and analytical results with the ratios between them. Figs. 18a to 18f illustrate the load–displacement curves for all experimental specimens and the corresponding analytical model.

From Table 9, it can be noticed that all F.E models gave a higher failure load compared to their counterparts in the experimental test except for model Col.00 (reference specimen). It can be observed that the percentage in failure load difference varies between 95% and 103% with an average of 98% and standard division about 2.65% only. When comparing displacement values at failure loads, a maximum difference of about 25% was observed between experimental and analytical results with mean value of 89% and standard division about 13.5%.

When comparing the load–displacement curves obtained from the experimental results with those obtained from the finite element models as shown in Fig. 18, an excellent match can be observed. The only difference is that the analytical results did not record the post-peak deformations after failure loads as shown in figure.

Conclusion

Based on the experimental and analytical results, the following conclusions may be made:

- Using steel jacketing techniques for strengthening RC columns has been proven to be effective since it increases the column capacity to a minimum of 20%.
- The failure mode of the control reinforced concrete column was brittle while strengthening with steel jacket changed failure mode to be more ductile.
- Specimen strengthened with angles or channel sections with batten plates recorded a higher failure load than that strengthened with plates.
- Increasing number of batten plates in 4L series did not help increasing failure load, while it increased failure load for 2C series.
- Using C-sections with batten plates or plates only in strengthening concrete columns needs cautions due to the buckling consideration of their thin thicknesses.
- 4L series encountered less deformation than other specimens.
- As the surface area of concrete covered by steel jacket increases the effect of confinement also increases.
- The simulation of strengthened RC columns using F.E analysis in ANSYS 12.0 [1] program is quite well since mode of failure, failure loads and displacements predicted were very close to those measured during experimental testing.
- For strengthened models, F.E package ANSYS 12.0 [1] overestimated failure loads compared to experimental results.

References

[1] ANSYS User Manual Revision 12.0, ANSYS Inc, Canonburg, Pennsylvania; 2009.
[2] R. Julio, P. Joaquín, A. Jose, C. Pedro, An experimental study on steel-caged RC columns subjected to axial force and bending moment, Eng. Struct. J. 33 (2010) 580–590.
[3] Khair B. Retrofitting of Square Reinforced Concrete Columns Subjected to Concentric Axial Loading with Steel Jackets, in: The Third Engineering Consultant work conference, Palestine, 2009.
[4] N. Pasala, S. Dipti, R. Durgesh, Seismic strengthening of RC columns using external steel cage, Earthquake Eng. Struct. Dyn. J. 38 (2009) 1563–1586.
[5] M. Rosario, P. Vincenzo, Reinforced concrete columns strengthened with angles and battens subjected to eccentric load, Eng. Struct. 31 (2008) 539–550.

[6] Willam J, Warnke P. Constitutive Model for Triaxial Behavior of Concrete, in: Seminar on Concrete Structures Subjected to Triaxial Stresses, International Association of Bridge and Structural Engineering Conference, Bergamo, Italy, 1974, p. 174.
[7] G. MacGregor, Reinforced Concrete Mechanics and Design, Prentice-Hall Inc, Englewood Cliffs, NJ, 1992.
[8] Damian K, Thomas M, Solomon Y, Kasidit C, Tanarat P. Finite Element Modeling of Reinforced Concrete Structures Strengthened with FRP Laminates. Report published under supervision of, Oregon Department of Transportation (ODOT) Research Group and Federal Highway Administration; 2001.